Scientia Iranica A (2012) 19 (4), 974–981

SCIENTIA IRANICA

Sharif University of Technology

Scientia Iranica

Transactions A: Civil Engineering

www.sciencedirect.com

An integrated ANN-GA for reliability based inspection of concrete bridge decks considering extent of corrosion-induced cracks and life cycle costs

A. Firouzi [a,*], **A. Rahai** [b]

[a] *Construction Engineering and Management Group, Science and Research Branch, Islamic Azad University, Tehran, 1477893855, Iran*

[b] *Department of Civil and Environmental Engineering, Amirkabir University of Technology, Tehran, P.O. Box: 15875-4413, Iran*

Received 6 April 2011; revised 15 February 2012; accepted 6 March 2012

KEYWORDS

Corrosion;
Concrete;
Random field;
Reliability;
Genetic algorithm;
Artificial neural network.

Abstract In most concrete bridge decks subject to deicing slats or constructed in chloride-laden environments, corrosion has caused serviceability damage in the form of severe cracking and/or spalling of the concrete cover. In this paper, whilst an analytical model is used for the simulation of corrosion induced crack width, random fields are utilized accounting for the spatial variability of the concrete material and environmental factors. Then, using the Monte Carlo simulation method, the extent of the damage is simulated as a dependent random variable during the service life of the bridge deck. Finally, for finding optimum reliability-based inspection plans, with minimum life cycle costs, an integrated Artificial Neural Network-Genetic Algorithm (ANN-GA) approach is proposed. The applicability of this method is investigated on a hypothetical bridge deck. It is concluded that the employed approach can well handle the high computational complexity of the problem in finding optimum inspection plans.

1. Introduction

Corrosion induced deterioration of RC structures, especially bridges, due to frequently applied deicing salts, is a main challenge to civil asset managers worldwide. Corrosion affects the reliability of RC structures, both in strength and serviceability limit states. In the past decade, many researchers worldwide have proposed various reliability based maintenance management systems. In these systems, mechanistic deterioration models are utilized in a probabilistic framework to account for temporal variations in material properties and loads as random variables [1].

In spite of considerable research accomplished on the reliability based maintenance planning of bridges, limited research exists in literature considering the spatial variability of the corrosion process. The fact that, in concrete structures, due to the spatial variability of workmanship and environmental factors, the material and dimensional properties are not homogeneous and, consequently, corrosion damage has a spatial variability, has motivated some researchers, e.g. [2–5], to study the effects of spatial variation on reliability models. These works revealed the usefulness of considering the spatial variability of corrosion parameters in prediction of the extent and likelihood of corrosion induced damage in RC structures. Most of these models assume that "failure" occurs when corrosion is initiated, or empirical models are used for prediction of the crack width increase with time. In the propagation phase, after initiation of surface cracking, their width will increase with time to a limit at which the spalling of concrete is prone. In recent years, several efforts have been made to model, analytically, the propagation phase of corrosion (e.g. [6–8]). In this paper, the model proposed by Li [8] is used for simulation of crack initiation and propagation with time [8].

The extent of damage is an important factor in actual repair and maintenance strategy selection. On the other hand, serviceability limit states, e.g. cracking, delamination, spalling, etc., in contrast to strength limit states, occur earlier in the

* Corresponding author. Tel.: +98 21 88980444.
E-mail addresses: firouzi@aut.ac.ir (A. Firouzi), rahai@aut.ac.ir (A. Rahai).

Peer review under responsibility of Sharif University of Technology.

ELSEVIER Production and hosting by Elsevier

1026-3098
doi:10.1016/j.scient.2012.06.002

Table 1: Statistical description of variables.

Variable	$\theta_x = \theta_x$ (m)	μ	COV	Distribution	Reference
Concrete cover (mm)	3.5	50	0.2	Normal	[11,12]
Concrete compressive strength, f_c, MPa	3.5	35	0.2	Lognormal	[11,12]
Surface chloride concentration (kg/m^3)	3.5	3.5	0.6	Lognormal	[11,12]
Critical chloride concentration (kg/m^3)	–	0.9	0.19	Uniform	[11,12]
Reinforcement size (mm)	–	12	–	–	[8]
Porous media around reinforcement (d_0), µm	–	12.5	–	–	[8]
α_{rust}	–	0.57	–	–	[8]
ρ_{rust} (kg/m^3)		3600	–	–	[8]
ρ_{steel} (kg/m^3)		7850	–	–	[8]
Poisson coefficient (ν)		0.18	–	–	[8]

service life of a bridge, and demand more for repair and maintenance interventions. So, the extent of cracked, spalled or delaminated areas (length) seems an appropriate indicator of bridge condition and reliability.

In most bridge management systems, routine inspections are mandatory, biannually. This is not only an expensive approach, but also in some congested traffic regions or severe environments, more frequent inspections may be necessary during the lifetime of the bridge. Suo and Stewart [9] showed the usage of data gathered during inspections in the updating of reliability models; this reveals the importance of well planned and timely inspections [9]. In this paper, a novel risk-based approach is presented considering the extent of damage and life cycle costs.

In this paper, a two-dimensional spatial–temporal variable reliability analysis is developed to predict the likelihood and extent of cracking for a RC deck top surface exposed to deicing slats. The spatial variability of parameters is modeled using random fields, discretized with a midpoint method. This model will consider the random spatial variability of concrete material properties, the concrete cover and surface chloride concentration. For risk-based repair and maintenance optimization, an integrated ANN-GA is proposed, in which acceptable levels of the extent of damage are considered. Such an inspection plan is put into effect, which yields minimum life cycle costs.

2. Corrosion mechanism

De-icing salts used in bridge decks cause ingress of chlorides through the concrete cover. The free chlorides in saturated concrete deactivate the natural protective oxide layer that is formed around the reinforcements by the strong alkalinity of the pore solution. Once the protective layer has dissolved, if chloride concentration exceeds a threshold value and enough oxygen and moisture are present, corrosion is initiated. In the propagation phase, since the corrosion products have a volume of three to six times greater than the original steel, tensile stresses within the concrete increase, which in turn result in cracking and spalling at the surface concrete. Numerous studies have found that the penetration of chlorides through concrete can be best represented by a diffusion process if the concrete is assumed to be relatively moist. In this case, the penetration of chlorides is given empirically by Fick's second law of diffusion, if the diffusion is considered as one-dimensional in a semi-infinite solid. Crank's solution to Fick's second law of diffusion is represented in Eq. (1) [10]:

$$C\,(x,t) = C_0 + (C_{sa} - C_0)\left[1 - \operatorname{erf}\left(\frac{x}{2\sqrt{D_a t}}\right)\right]. \tag{1}$$

In general, the chloride concentration profiles obtained under different climates are used in mathematical models for obtaining parameters of Eq. (1). A plot of chloride concentration vs. penetration depth can often be closely described by Crank's solution to Fick's second law of diffusion. The curve-fitting results in these parameters: apparent diffusion coefficient, D_a, apparent surface chloride concentration, C_{sa}, and the original chloride concentration, C_0, then $C\,(x,t)$ express the chloride content at a depth of x at time t. The corrosion of reinforcements is initiated when the chloride content, in steel bar embedment depth, X_c, exceeds a threshold value, C_{cr}, which depassivates the steel embedded in the concrete, provided that sufficient moisture and oxygen are present, The corrosion initiation time (T_{int}) can be calculated using Eq. (2) as follows:

$$T_{\text{int}} = \frac{X_c{}^2}{4D_a}\left[\operatorname{erf}^{-1}\left(\frac{C_{\text{cr}} - C_0}{C_{sa} - C_0}\right)\right]^{-2}. \tag{2}$$

In general, the uncertainty of governing parameters can be handled with random variables. Although accurate statistical distributions cannot be derived without sufficient experimental data from existing structures, Dupart [11], having studied various measurements in the literature for various environmental and workmanship classifications, made some general propositions [11]. Based on such propositions, the descriptive parameters of random fields and random variables are as in Table 1.

For reliability calculations, a closed form mathematical model has a paramount advantage. In this paper, the analytical model developed by Li et al. [8] is used for simulation of the corrosion-induced crack width variation with time. The merit of this model is that it is directly related to factors that affect corrosion, such as concrete geometry and property, and corrosion rate [8].

In this model, as shown schematically in Figure 1, concrete with embedded reinforcing steel bars is modeled as a thick-wall cylinder, where d_0 is the thickness of the annular layer of concrete pores (that is, a pore band) at the interface between the steel bars and concrete, D is the diameter of the steel bar, and X_c is the concrete cover.

The inner and outer radii of the thick-wall cylinder are $a = (D + 2d_0)/2$ and $b = X_c + (D + 2d_0)/2$. When the steel bar corrodes in concrete, its products fill the pore band completely and a ring of corrosion products forms, the thickness of which, $d_s(t)$ (Figure 1), can be determined from Eq. (3), as follows [6]:

$$d_s\,(t) = \frac{W_{\text{rust}}(t)}{\pi\,(D + 2d_0)}\left(\frac{1}{\rho_{\text{rust}}} - \frac{\alpha_{\text{rsut}}}{\rho_{st}}\right), \tag{3}$$

where α_{rust} is a coefficient related to the types of corrosion product, ρ_{rust} is the density of corrosion products, ρ_{st} is the density of steel, and $W_{\text{rust}}(t)$ is the mass of corrosion products.

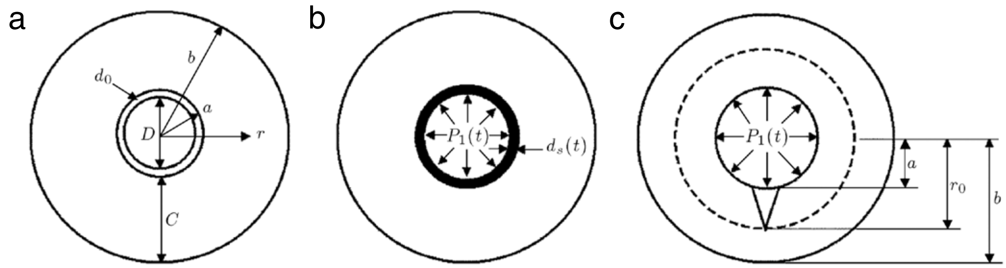

Figure 1: Schematic representation of cracking process [8].

$W_{\text{rust}}(t)$ increases with time and can be determined from Eq. (4) [6]:

$$W_{\text{rust}}(t) = \left(2\int_0^t 0.105\,(1/\alpha_{\text{rust}})\,\pi D \times i_{\text{corr}}(t)\,dt\right)^{1/2}, \tag{4}$$

where $i_{\text{corr}}(t)$ is the corrosion current density (in μA/cm^2). In general, the formation of rust products on the steel surface will reduce the diffusion of the iron ions away from the steel surface, resulting in reduced corrosion rates with time. For example, Vu et al. [12] suggested the following time dependent equation for $i_{\text{corr}}(t)$ [12]:

$$i_{\text{corr}}(t) = i_{\text{corr}}(1) \times 0.85\,(t - T_{\text{int}})^{-0.3}, \tag{5}$$

where T_{int} is the time to corrosion initiation and $i_{\text{corr}}(1)$ is the corrosion current density in the first year after corrosion initiation, which is based on concrete quality and water to cement ratio, and can be calculated using Eq. (6) as follows:

$$i_{\text{corr}}(1) = \frac{27(1 - w/c)^{-1.64}}{X_c}. \tag{6}$$

According to Li et al. [8], the growth of the ring of corrosion products exerts an outward pressure on the concrete at the interface between the rust products and concrete [8]. Under this expansive pressure, the concrete cylinder undergoes three phases in the cracking process:

(1) Not cracked,
(2) Partially cracked, and
(3) Completely cracked.

In phase 1 (no cracking), the concrete can be considered as elastically isotropic, so that the theory of elasticity can be used to determine the stress and strain distribution in the cylinder. For a partially cracked concrete cylinder, cracks are considered to be smeared and the concrete to be a quasi-brittle material, so that the stress and strain distribution in the cylinder can be determined based on fracture mechanics. When the crack penetrates through to the concrete surface, the concrete cylinder fractures completely. Knowing the distribution of stress and strain, the crack width at the surface of the concrete cylinder can be determined as follows [8]:

$$w_c = \frac{4\pi d_s}{(1-\nu_c)\,(a/b)^{\sqrt{\alpha}} + (1+\nu_c)\,(b/a)^{\sqrt{\alpha}}} - \frac{2\pi b f_t}{E_{ef}}, \tag{7}$$

where ν_c is Poisson's ratio of concrete and α (<1) is the tangential stiffness reduction factor. According to Li et al., it is assumed that the residual tangential stiffness is constant along the cracked surface, that is at the interval $[a, r_0]$ and represented by E_{ef}, where E_{ef} is the effective elastic modulus of concrete, which can be calculated as per Eq. (8), where φ_{cr} and E_c represent the creep coefficient and elastic modulus of the concrete [6]:

$$E_{ef} = \frac{E_c}{1 + \varphi_{\text{cr}}}. \tag{8}$$

In Eq. (7), the key variables are the thickness of corrosion products, d_s, which is directly related to the corrosion rate (i_{corr}), and the stiffness reduction factor, α, which is related to stress conditions and the concrete property and geometry. Eq. (7), which is used in this paper, has been verified by both numerical and experimental results [8]. In using this equation, one needs to calculate the time dependent variables, α and d_s. The former is determined solving simultaneous equations derived in Ref. [8], which are not repeated here for briefness purposes, while the latter is calculated according to Eq. (3).

The various mechanical properties of concrete are usually correlated to its compressive strength; a parameter which can be easily measured in practice. Referring to ACI 318-08 [13], the concrete tensile strength and modulus of electricity are related to compressive strength as [13]:

$$\text{Concrete Tensile Strength: } f_t = 0.53\sqrt{f_c'}\ \text{(MPa)}, \tag{9}$$

$$\text{Concrete Modulus of Elasticity: } E_c = 4600\sqrt{f_c'}\ \text{(MPa)}. \tag{10}$$

The other important influencing parameter in studying corrosion in RC structures is the chloride diffusion coefficient. In this paper, the model developed by Papadakis et al. [14] is used [14], which is represented as:

$$D_a = D_{\text{H}_2\text{O}} 0.15 \frac{1 + \rho_c \frac{c}{w}}{1 + \rho_c \frac{w}{c} + \frac{\rho_c}{\rho_a}\frac{a}{c}} \left(\frac{\rho_c \frac{w}{c} - 0.85}{1 + \rho_c \frac{w}{c}}\right)^3. \tag{11}$$

In this model, a/c is the aggregate-to-cement ratio, ρ_c and ρ_a are the mass densities of cement and aggregates, respectively, and $D_{\text{H}_2\text{O}}$ is the chloride diffusion coefficient in an infinite solution (=1.6×10^{-5} cm^2/s for NaCl). The water–cement ratio is estimated from Bolomey's formula for Ordinary Portland Cement (OPC) concretes as follows:

$$w/c = \frac{27}{f_c' + 13.5}, \tag{12}$$

where f_c' is the concrete compressive strength of a standard test cylinder in MPa.

3. Neural networks

Artificial Neural Networks (ANNs) are models based on the neural structure of the brain. During the last decade, approximations based on the concept of artificial neural networks are being introduced into reliability analysis. The primary motivation of using neural networks lies in their capability for

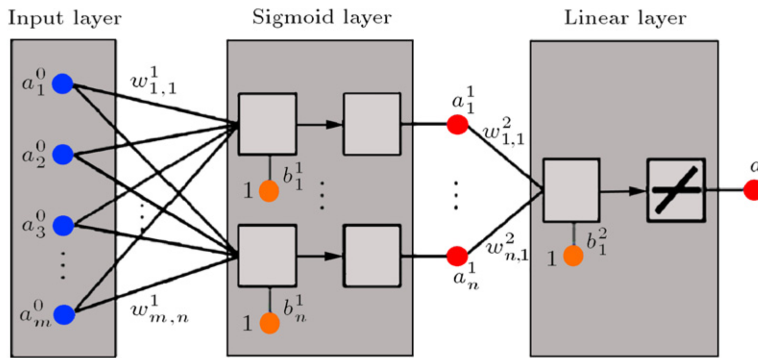

Figure 2: Feed forward neural network architecture [18].

good approximation of the results of time consuming repeated analyses of the Monte Carlo method. Papadrakakis et al. [15] examined the utility of neural networks in the reliability analysis of elastic–plastic structures and found this method very attractive [15]. Hurtado and Alvarez [16] compared the performance of various types of neural network in structural reliability analyses [16]. Hurtado [17] demonstrated the applicability of Neural Networks for analyzing uncertainty in one dimensional stochastic finite element problems [17]. Most and Bucher [18] used a 2-D random field for representation of fluctuating material properties and then employed neural networks for approximation of the response of a complicated model of coupled meshless and finite element analysis [18].

There exist a variety of alternatives to design a neural network. The focus of this study is on feed forward neural networks, which are already applied successfully in many fields of engineering. In Figure 2, a general schematic structure of this kind of neural network is illustrated. In this work, the neural network approach is employed to obtain expected life cycle costs with time during the service life of a hypothetical bridge deck. A commercially available software package, MATLAB Neural Network toolbox, is employed to facilitate the analysis. Back-propagation has generally been the most popular method used to train nonlinear, multi-layered neural networks to perform function approximation and pattern classification. Hence, three layer back-propagation neural networks are used here. It has been shown that ANNs, with one hidden layer, can approximate any function, given that sufficient degrees of freedom are provided. Whilst, in the hidden layer on each neuron, the sigmoid transfer function is used, a linear function is employed for the output layer. The back-propagation learning rule is used to adjust the weights and biases of the network in order to minimize the mean squared error between the resultant values, solving the equations of the analytical model and those predicted from the neural network model. The minimization of the mean squared error proceeds until it converges to a preset tolerance for all test datasets.

A very important point for sufficient network approximation is the design of the network architecture. Depending on the number of available training samples, the number of neurons in the hidden layers has to be chosen in such a way that so-called over-fitting is avoided. This phenomenon occurs if the number of hidden nodes is too large for the number of training samples. Then, the network can converge more easily and fits well for the training data, but it cannot generalize well for other data. Hagan [19] suggested that the number of training samples, m, should be larger than the number of adjustable parameters [19]:

$$(n+2)M+1<m, \tag{13}$$

where n is the number of input values and M is the number of hidden neurons for a network with a single hidden layer.

The selection of training datasets is an important issue in the context of establishment of the ANN model. The main aim in the selection of training datasets is to make the selected training data as uniform as possible to cover the entire design space. In this study, the time intervals between successive inspections are the decision variables of the optimization problem. Every inspection plan can be represented with a binary vector, $\boldsymbol{t}$, whose dimension equals the service life of the bridge; 1's represents inspection implementation during a lifetime. Because of the complexity of the problem, the test datasets, e.g., inspection plan vectors, are generated at random with respect to the constraints of Eqs. (15h)–(15j).

4. The proposed methodology

The proposed method is presented on a hypothetical bridge deck. Monte Carlo simulation of random fields requires extensive computational effort. In this section, the proposed algorithm is briefly described in a step by step manner and then the results of the analysis are presented:

4.1. Discretization of random fields

A spatial time-dependent reliability analysis is developed for a hypothetical RC bridge deck 12 m in length and 10 m in width exposed to de-icing salts. The analysis considers corrosion initiation and then the propagation of corrosion-induced upper cover cracking, until a crack width of 0.3 mm is reached, which is the prescribed crack width limit in [20] for severe cracking [20]. A 2D random field is applied to the RC bridge deck considering the spatial variability concrete compressive strength. This means that related properties of concrete, e.g. the chloride diffusion coefficient, concrete tensile strength, the concrete effective modulus of elasticity, water–cement ratio and corrosion density rate, are dependent random fields of the compressive strength of concrete. Furthermore, concrete cover depth and surface chloride concentration are represented with random fields to account for spatial variations of these parameters.

Using a midpoint method, the 2D random field is discretized into square elements of size Δ, resulting in N_T statistically correlated elements. There exist various discretization methods, from which the midpoint method is simple and accurate enough for random fields with a large scale of fluctuations. Sudret and Der Kiureghian [21] presented a full description of random fields [21]. For every realization of the Monte Carlo

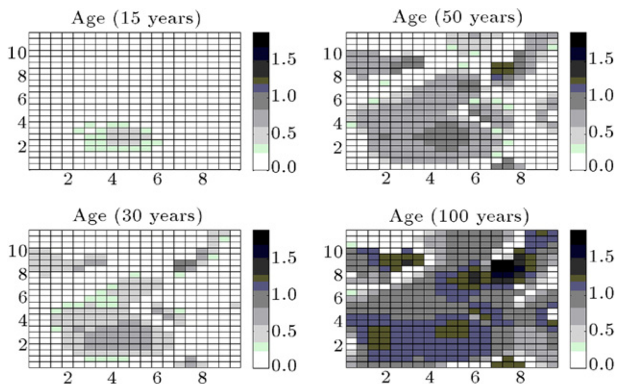

Figure 3: Random realization of spatial variation of crack width increase with time.

simulation, the proportion of the deck area with crack widths exceeding the limit crack width at the time of t is calculated as follows:

$$X(t) = \frac{n_f\left[t > T\mathrm{int}(j) + Tsc(j)\right]}{N_T}. \quad (14)$$

In Eq. (14), the corrosion initiation time of element j is denoted by $T\mathrm{int}(j)$. This element's crack width reaches 0.3 mm in $Tsc(j)$ years after corrosion initiation, and n_f is the total number of elements for which the condition $[t > T\mathrm{int}(j) + Tsc(j)]$ is true.

According to Stewart and Mullard [22], the scale of fluctuation of these random fields is approximately 3.5 m ($d_x = d_y = 2.0$ m) [22].

In Table 1 full statistical descriptions of random fields, random variables and deterministic variables are illustrated. Using the midpoint method, the 2D random field is discretized into square elements of size $\Delta = 0.5$ m, resulting in $N_T = 480$ elements.

For simulation of the discretized random fields and prediction of the crack width propagation in the hypothetical bridge deck, a MATLAB code is developed. The developed code in MATLAB carries out Monte Carlo simulation in the space of independent standard normal variables of discretized random fields. For example, Figure 3 illustrates a random realization of the simulated crack width of discretized elements of the studied deck during a lifetime. After N_{sim} realization of the simulation process, $X(t)$, as the dependent random variable can be simulated during a predetermined lifetime. The extent of damage increases with time, and the RC deck cannot meet the designed service life without repair.

4.2. Computational procedure

The main purpose of this paper is to present a step by step method for finding the optimum risk-based inspection plans, considering the extent of damage, which yields to minimum lifetime inspection and maintenance costs. In this regard, the capabilities of an integrated ANN-GA is investigated. Below is the step by step computational procedure:

Step 1—Use the midpoint method for discretization of random fields into N_T correlated random variables.

Step 2—Simulate N_{sim} realization of correlated random variables.

Step 3—Calculate corrosion initiation time, T_{int}, for every discretized element in every realization of the simulation using Eq. (2).

Step 4—Calculate the crack initiation time and crack width of every decartelized element during a prescribed lifetime of the deck in every realization of the simulation, using Eq. (7), and solving simultaneous equations.

Step 5—Calculate extent of the severely cracked area of the deck in every realization of the simulation, e.g. crack width greater than limit crack width, using Eq. (14).

Step 6—Randomly produce m inspection plans, e.g. $\boldsymbol{t}$ vectors, during a prescribed lifetime of the deck.

Step 7—Calculate expected life cycle maintenance and inspection cost for every random inspection plan.

Step 8—Train neural network for simulation of expected life cycle costs for every inspection plan.

Step 9—Use trained neural network as a surrogate for the time-consuming event based Monte Carlo simulation for calculation of expected inspection and maintenance life cycle costs.

Step 10—Use a genetic algorithm for finding the optimum or near optimum inspection plan that yields to the minimum present value of the lifetime inspection and maintenance costs.

The initial steps 1–5 result in a simulated extent of damage without any repair intervention, whilst steps 6–10 include procedures for optimization of inspection plans.

4.3. Formulation of the optimization problem

Based on spatial time dependent reliability analysis, the propagation of the extent of damage with time can be simulated. As per above results, the RC deck cannot meet the designed service life without repair. In reality, some areas of the deck will undergo earlier deterioration and, hence, will be repaired first. The remaining parts of the deck and even the repaired areas will continue to deteriorate and will likely need repair at later times. It is assumed in this paper that the bridge will be inspected and, at every inspection, if the extent of damage is more than an acceptable threshold, it will be repaired. Furthermore it is assumed that repaired areas will be brought to an undamaged new condition. Decisions about the selection of optimum inspection and maintenance strategies shall be based on minimum life cycle costs.

Since the repair actions depend on previously failed elements, and the history of failure is not evident, deriving a closed form formula for this problem is cumbersome. In this paper, an event-based Monte Carlo simulation is conducted. The discounted present value of repair and maintenance costs are calculated in every simulation run and expected total costs are considered as the criterion for decision making. It should be noted that for simplicity, other costs, especially user costs, during repairs is not considered in the analysis.

The minimum threshold of the repair and critical crack width are of paramount importance in decision analysis. In this analysis, $X_{\mathrm{rep}}^{\min}$ corresponds to the threshold at which repairs are accomplished. It should be noted that the repair threshold, $X_{\mathrm{rep}}^{\min}$, may reach a time between two succeeding inspection periods. Apparently, it will not be detected until it is inspected and, consequently, the difference between the repaired area after inspection and the repair threshold will increase. One should consider the fact that delaying inspection, despite lowering the present value of life cycle costs, increases the risk of failure. The maximum tolerable extent of damage, $X_{\mathrm{rep}}^{\max}$, is introduced in this analysis to prevent an unacceptable extent of damage during the lifetime of the bridge deck. Finally, the optimization problem may be formulated as:

$$\text{Min } Z = E\left(LCC(t)\right), \tag{15a}$$

Subject to:

$$E(LCC) = PRC_{\text{ins}} + E\left(PRC_{\text{rep}}\right), \tag{15b}$$

$$PRC_{\text{ins}} = \sum_{i=1}^{Nins} \frac{C_{\text{ins}}(i)}{(1+r)^{Ti}}, \tag{15c}$$

$$E\left(PRC_{\text{rep}}\right) = \frac{\sum_{k=0}^{N_{\text{sim}}} \sum_{j=1}^{Nrep} \frac{C_{\text{rep}}(k,j)}{(1+r)^{T(k,j)}}}{N_{\text{sim}}}$$

$$\text{for } j = 1 \text{ to } N_{\text{rep}} \text{ and } k = 1 \text{ to } N_{\text{sim}}, \tag{15d}$$

$$C_{\text{rep}}(k,j) = \left(5000 + 2000 \times \left(X_{k,j} \times A_T\right)\right) \text{€}$$

$$\text{for } j = 1 \text{ to } N_{\text{rep}} \text{ and } k = 1 \text{ to } N_{\text{sim}}, \tag{15e}$$

$$C_{\text{ins}}(i) = 5000\,\text{€} \quad \text{for } i = 1 \text{ to } N_{\text{ins}}, \tag{15f}$$

$$X_{\text{rep}}^{\min} \le X_{k,j} \le X_{\text{rep}}^{\max}, \tag{15g}$$

$$1 \le t_i \le 5 \text{ years} \quad \text{for } i = 1 \text{ to } N_{\text{ins}}, \tag{15h}$$

$$T_i = T_{i-1} + t_i \quad \text{for } i = 1 \text{ to } N_{\text{ins}}, \tag{15i}$$

$$T_{N_{\text{ins}}} \le 50 \text{ years}, \tag{15j}$$

$$N_{\text{rep}} \le N_{\text{ins}}, \tag{15k}$$

$$N_{\text{ins}} \le 50. \tag{15l}$$

This optimization problem, because of its high complexity, cannot be solved except with Artificial Intelligence (AI) techniques. In the following section, the application of an integrated ANN-GA is presented.

4.4. Analysis

The motivation behind employing neural networks is their capability of function approximation. In this paper, for calculation of the crack width of every discretized element at every annual time step, a couple of simultaneous nonlinear equations shall be solved. This process shall be repeated for N_{sim} times to simulate $X(t)$ before repair interventions. In reference to Figure 3, in every realization of Monte Carlo simulation, one can expect a different spatial and temporal variation of damage and, consequently, the extent of damage increases with time, e.g. $X(t)$. In Figure 4, the efficiency of an inspection plan in lowering the extent of damage and the corresponding incurred costs during a life cycle is schematically presented on a randomly selected realization of a Monte Carlo simulated bridge deck.

It is obvious during a lifetime that very different inspection plans, $\boldsymbol{t}$, are possible. The following ANN-GA algorithm is proposed for finding the optimum inspection plan, $\boldsymbol{t}_{\text{opt}}$, which yields to minimum expected life cycle costs.

The life cycle cost of 1000 randomly initiated inspection plans is calculated. Then, a three layer feed forward neural network is trained for calculation of the life cycle costs of any inspection plan. The problem is solved for 50 years of service life, resulting in 50 neurons in the input layer. In every inspection plan, $\boldsymbol{t}$, the Ones (1's) represent the inspection being conducted on those ages of the deck, and Zeros (0's) mean no inspection will be performed on the corresponding age. Apparently, in the output layer, there is just one neuron simulating the expected life cycle cost of every inspection plan,

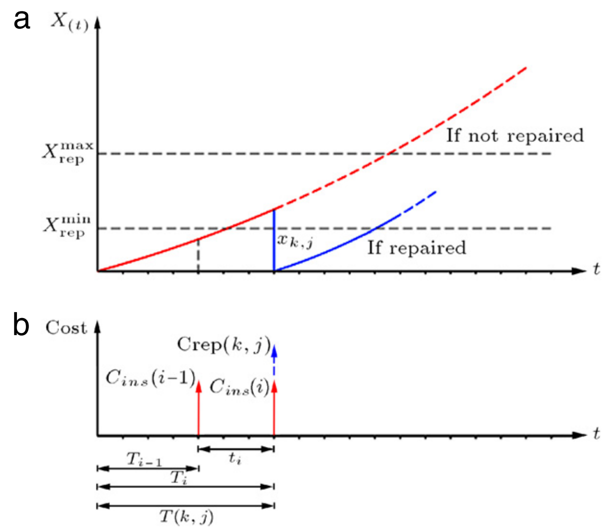

Figure 4: The effect of a random inspection plan on random realization of simulated extent of damage.

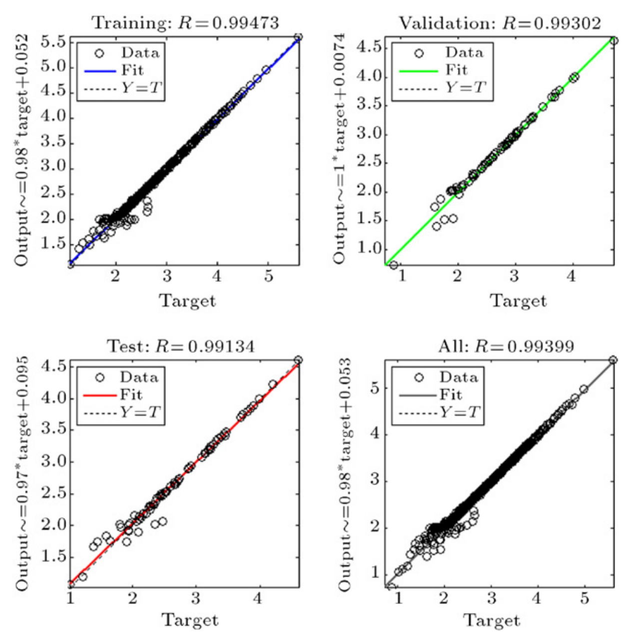

Figure 5: Correlation between ANN results and Monte Carlo simulation.

e.g. $E(LCC(t))$. Finally, the number of hidden layer neurons is determined, based on trial and error, to reach the minimum Mean Square Error (MSE) of the network, and an acceptable R-factor of validation and test datasets after training. With respect to Eq. (13) and the aforementioned considerations, a 50-50-1 (Input-Hidden-Output) structure of the network is finalized. The activation functions of hidden and output layers are sigmoid and linear, respectively.

Figure 5 illustrates that trained NN has a very good approximation capability, because the R factors in all three groups of data, e.g. training, validation and testing, are above 0.98.

The trained NN can be used as a surrogate for the time-consuming and inefficient event based Monte Carlo simulation.

At the final step, for finding the optimum inspection plans of the optimization problem (Eq. (15)), the utility of GA as a

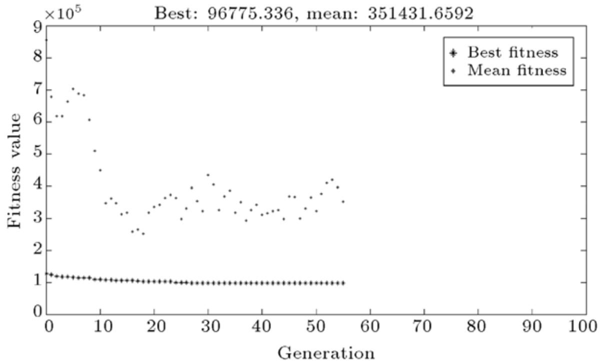

Figure 6: Best fitness of genetic algorithm optimization.

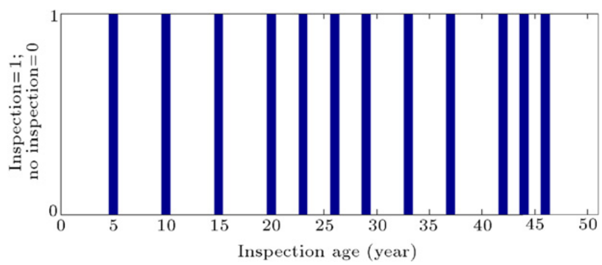

Figure 7: Optimum inspection time intervals using genetic algorithm.

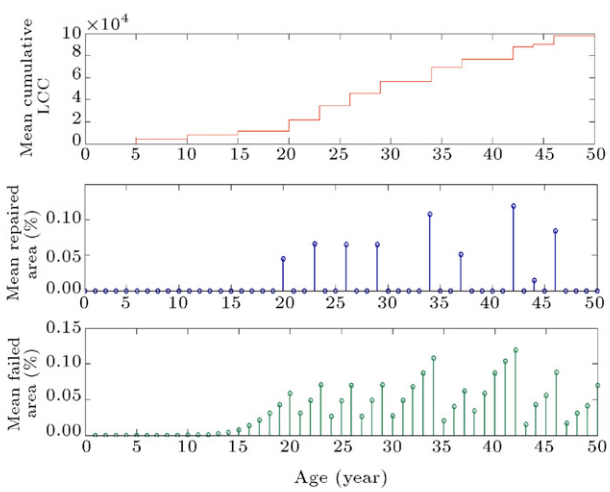

Figure 8: Optimum inspection plan. (a) Mean percent of failed area; (b) mean percent of repaired area; and (c) expected *PRV* of *LCC*..

global search method is investigated. A binary code, GA, using the MATLB GA toolbox, is examined here. Based on the final tuned parameters of the GA, population size equals 200, the mutation function is uniform with a 0.05 rate, the cross over fraction is 0.8 and the elite count is 5 in every generation. For illustration, the problem is solved for X_{rep}^{min} and X_{rep}^{max} equal to 5% and 30% of the total deck area.

In Figure 6, the convergence of the algorithm is presented. In this example, the algorithm stops after 55 generations because the best fitness of this generation is halt for 5 consecutive generations.

The corresponding best individual (solution) is illustrated in Figure 7. As predicted in the first years of the bridge deck service, in this example, until after 20 years of service, the expected extent of damage is low (less than X_{rep}^{min}) and there is no need for repairs. Consequently, the time intervals of successive inspections are 5 years; the maximum allowable time interval as per Eq. (15h). But, when the damage extent and severity propagates with time (between 20 and 29 years), as illustrated in Figure 8(a), the bridge manager shall allocate enough budget for more frequent inspections and repairs for lowering the risk of serviceability failure, meaning the extent of severely cracked areas are more than X_{rep}^{max}. According to Figure 8(a) and (b), during this period of life, inspection and repair should be conducted 4 times. These interventions will remedy the bridge condition and, subsequently, between the ages of 30 and 41, less stringent interventions will be required. The other interesting conclusion is the need for successive repairs after being in-service for an adequately long time. This can be explained with due attention to the fact that the initiation phase of corrosion, in contrast to the propagation phase, governs the service life of the affected concrete structures. In other words, if, in a reinforced concrete element, corrosion is initiated, the occurrence of cracking is expected just within a few years. In this example, the mean simulated corrosion initiation time is 35 years, and the propagation to limit the 1 mm crack width occurs in 45.5 years. It means that most unrepaired areas will undergo corrosion, and cracking will be manifested in these areas of deck more frequently between the ages of 42 and 50 years. In Figure 8(c), the present value (*PRV*) of the optimum expected life cycle inspection and maintenance costs is illustrated.

5. Conclusion

The extent of damage, as an indicator of the bridge deck condition, is an appropriate parameter in decision making, regarding repair and maintenance intervention. Spatial variation of material and environmental factors affects the corrosion process in RC structures and, consequently, the location and extent of the damage is a spatially dependent variable. For simulation of the spatial variation of the corrosion process, random fields are utilized. Since the midpoint method is computationally efficient, it is used for discretization of random fields. In this paper, after simulation of the extent of damage, the usefulness of artificial intelligence methods is investigated in the risk-based inspection planning of bridge decks. As presented, the problem of finding an inspection plan that yields to the minimum expected life cycle cost is computationally very complex. On the other hand, solving this problem is very rewarding for developning practical bridge maintenance management systems. The usefulmess of an integrated ANN-GA approach is examined on a hypothetical bridge deck, and an optimum inspection plan is sought with this algorithm. A three layer feed forward ANN is used for simulation of the expected life cycle costs of various inspection plans. The correlation coefficients were found to be 99%, 99% and 99% for training, validation and testing datasets, respectively, which shows the accuracy of the results obtained with trained ANN working as a sorrugate for the inefficient and time-consuming event based Monte Carlo simulation. Finally, the global optimum searching capability of the genetic algorithm makes it possible for inspection intervals during the lifetime of the bridge deck to be planned in such a way that the total expected life cycle costs are minimum, while the extent of repaired damage in every intervention is within a minimum threshold of repair initiation, and a maximum tolerable extent of damage. The proposed algorithms handles the high complexity of the problem and the results are in good agreement with practical experience.

6. Notation

The following notation is used throughout this paper:

$LCC(t)$: Life cycle cost of inspection plan with the inspection plan conducted at the time intervals of $t = (t_1, t_2, \ldots, t_i, \ldots, t_{N_{\text{ins}}})$,
$C_{\text{ins}}(i)$: Inspection cost conducted on age $T(i)$ of the bridge deck
$C_{\text{rep}}(k, j)$: Cost of repair intervention conducted on age $T(k, j)$ of the bridge deck in the kth simulation
$X_{\text{rep}}^{\text{min}}$: Threshold extent of damage to conduct repairs
$X_{k,j}$: Extent of repaired damage on age $T(k, j)$ of the bridge dec k in the kth realization of simulation
$X_{\text{rep}}^{\text{max}}$: Maximum tolerable extent of damage before repairs
t_i: Time interval between inspections
N_{ins}: Total number of inspections
T_i: Age of bridge on the ith inspection
$T(k, j)$: Age of bridge on the jth repair intervention on the kth realization of simulation
N_{rep}: Total number of repair interventions during the lifetime of the bridge deck
N_{sim}: Number of realizations of simulation
N_T: Number of discretized elements
PRC_{ins}: Present value of total inspection costs during the lifetime of the bridge deck
PRC_{rep}: Present value of total repair costs of every realization of simulation
$E(g)$: Expected value of variable; g.

References

[1] Frangopol, D.M., Kong, J. and Gharaibeh, E. "Reliability-based life-cycle management of highway bridges", *ASCE J. Comput. Civil Eng.*, 15(1), pp. 27–34 (2001).
[2] Li, Y., Vrouwenvelder, T., Wijnants, G.H. and Walraven, J. "Spatial variability of concrete deterioration and repair strategies", *Struct. Concr.*, 5(3), pp. 121–130 (2004).
[3] Stewart, M.G., Mullard, J.A., Drake, B.J. and Al-Harthy, A.S. "Utility of spatially variable damage performance indicators for improved safety and maintenance decisions of deteriorating infrastructure", *Civ. Eng. Environ. Syst.*, 24(2), pp. 149–163 (2007).
[4] Karimi, A.R., Ramachandran, K. and Buenfeld, N. "Probabilistic analysis of reinforcement corrosion with spatial variability using random field theory", *Proceedings of the Ninth International Conference on Structural Safety and Reliability, ICOSSAR 05*, Rome, Italy (2005).
[5] Sudret, B. "Probabilistic models for the extent of damage in degrading reinforced concrete structures", *Reliab. Eng. Syst. Saf.*, 93, pp. 410–422 (2008).
[6] Liu, Y. and Weyers, R.E. "Modeling the time-to-corrosion cracking in chloride contaminated reinforced concrete structures", *ACI Mater. J.*, 95(6), pp. 675–681 (1998).
[7] El Maaddawy, T. and Soudki, K. "A model for prediction of time from corrosion initiation to corrosion cracking", *Cem. Concr. Compos.*, 29(3), pp. 168–175 (2007).
[8] Li, C.Q., Melchers, R.E. and Zheng, J.J. "Analytical model for corrosion-induced crack width in reinforced concrete structures", *ACI Struct. J.*, 103(4), pp. 479–487 (2006).
[9] Suo, Q. and Stewart, M.G. "Corrosion cracking prediction updating of deteriorating RC structures using inspection information", *Reliab. Eng. Syst. Saf.*, 94(8), pp. 1340–1348 (2009).
[10] American Concrete Institute, *ACI 365 1R-00* "Service life prediction, state of the art report", Detroit, USA (2000).
[11] Duprat, F. "Reliability of RC beams under chloride ingress", *Constr. Build. Mater.*, 21, pp. 1605–1616 (2007).
[12] Vu, K., Stewart, M.G. and Mullard, J. "Corrosion-induced cracking: experimental data and predictive models", *ACI Struct. J.*, 102(5), pp. 719–726 (2005).
[13] American Concrete Institute, Building Code Requirements for Structural Concrete, ACI 318-05, Detroit (2008).
[14] Papadakis, V.G., Roumeliotis, A.P., Fardis, M.N. and Vagenas, C.G. "Mathematical modeling of chloride effect on concrete durability and protection measures", In *Concrete Repair, Rehabilitation and Protection*, R.K. Dhir and M.R. Jones, Eds., pp. 165–174, E&FN Spon, London, UK (1996).
[15] Papadrakakis, M., Papdopoulis, V. and Lagaros, N.D. "Structural reliability analysis of elastic–plastic structures using neural networks and Monte Carlo simulation", *Comput. Methods Appl. Mech. Engrg.*, 136, pp. 145–163 (1996).
[16] Hurtado, J.E. and Alvarez, D.A. "Neural network based reliability analysis: a comparative study", *Comput. Methods Appl. Mech. Engrg.*, 19, pp. 113–132 (2001).
[17] Hurtado, J.E. "Analysis of one-dimensional stochastic finite elements using neural networks", *Probab. Eng. Mech.*, 17, pp. 35–44 (2002).
[18] Most, T. and Bucher, C. "Probabilistic analysis of concrete cracking using neural networks and random fields", *Probab. Eng. Mech.*, 22, pp. 219–229 (2007).
[19] Hagan, M.T., Demuth, H. and Beale, M., *Neural Network Design*, PWS Publishing Company (1996).
[20] Duracrete "Final technical report: probabilistic performance based durability design of concrete structures", The European Union—Brite EuRam III (2000).
[21] Sudret, B. and Der Kiureghian, A. "Stochastic finite element methods and reliability: a state of the art report", Report No. UCB/SEMM, Department of Civil and Environmental Engineering University of California, Berkeley (2000).
[22] Stewrat, M.G. and Mullard, J.A. "Spatial time-dependent reliability analysis of corrosion damage and the timing of first repair for RC structures", *Eng. Struct.*, 29(7), pp. 1457–1464 (2007).

Afshin Firouzi graduated from Sharif University of Technology (SUT) with a B.S. degree in Civil Engineering and pursued his graduate studies in Amirkabir University of Technology (AUT) in the field of Construction Engineering and Management. He graduated with a Ph.D. degree from AUT in 2010. Currently, he works as Assistant Professor in the Construction Engineering and Management Group of the Islamic Azad University, Science and Research Branch, Tehran, Iran. His primary research interests are infrastructure management, construction engineering and project management, structural reliability and risk management and advanced concrete technology.

Alireza Rahai obtained a B.S. degree in 1975 from Amirkabir University of Technology, Tehran, Iran, and a Ph.D. degree in the field of Structural Engineering from the University of Paris, France, in 1979. Since 1980, he has been cooperating with Amirkabir University of Technology (AUT) as Professor in the Department of Civil Engineering. His research interests include concrete structures, innovative construction materials and application of FRP composites in retrofit of structures.